The published version can be found on the Royal Society of Chemistry´s webpage at
http://dx.doi.org/10.1039/C3CP50548K

N-site de-methylation in pyrimidine bases as studied by low energy electrons and *ab initio* calculations

D. Almeida [1], D. Kinzel [2], F. Ferreira da Silva [1], B. Puschnigg [3], D. Gschliesser [3], P. Scheier [3], S. Denifl [3,*], G. García [4,5], L. González [2] and P. Limão-Vieira [1,*]

[1] Laboratório de Colisões Atómicas e Moleculares, CEFITEC, Departamento de Física, Faculdade de Ciências e Tecnologia, Universidade Nova de Lisboa, 2829-516 Caparica, Portugal
[2] Institut für Theoretische Chemie, Universität Wien, Währinger Strasse 17, A-1090 Wien, Austria
[3] Institut für Ionenphysik und Angewandte Physik and Center of Molecular Biosciences Innsbruck, Universität Innsbruck, Technikerstr. 25, A-6020 Innsbruck, Austria
[4] Instituto de Física Fundamental, Consejo Superior de Investigaciones Científicas, Serrano 113-bis, 28006 Madrid, Spain
[5] Departamento de Física de los Materiales, UNED, Senda del Rey 9, 28040 Madrid, Spain

Abstract

Electron transfer and dissociative electron attachment to 3-methyluracil (3-meU) and 1-methylthymine (1-meT) yielding anion formation have been investigated in atom-molecule collision and electron attachment experiments, respectively. The former has been studied in the collision energy range 14-100 eV whereas the latter in the 0-15 eV incident electron energy range. In the present studies, emphasis is given to the reaction channel resulting in the loss of the methyl group from the N-sites with the extra charge sitting on the pyrimidine ring. This particular reaction channel has neither been approached in the context of dissociative electron attachment nor in atom-molecule collisions yet. Quantum chemical calculations have been performed in order to provide some insight into the dissociation mechanism involved along the N-CH_3 bond reaction coordinate. The calculations provide support to the values derived from the electron transfer measurements, allowing for a better understanding of the role of the potassium cation as a stabilising agent in the collision complex. The present comparative study

gives insight into the dynamics of the decaying transient anion and more precisely, into the competition between dissociation and auto-detachment.

Keywords: 1-methylthymine, 3-methyluracil, electron transfer, negative ion formation, dissociative electron attachment, atom-molecule collisions, TOF mass spectrometry, ab initio calculations

* Corresponding authors. Fax: +43 512 507 2932; Fax: + 351 21 294 85 49
Email addresses: stephan.denifl@uibk.ac.at (S. Denifl); plimaovieira@fct.unl.pt (P. Limão-Vieira)

1. Introduction

In the context of radiation damage to biologically relevant systems, gas-phase dissociative electron attachment (DEA) studies have thoroughly shown that radiation-induced damage to DNA, along with its ensuing long-term biological consequences, can be attributed to underlying fundamental physical and chemical degradation mechanisms. These processes occur during the initial stages of the interaction between the radiation and the molecules that constitute the biological environment[1,2]. For each 1 MeV of incident primary radiation, along the ionisation track an estimated amount of ~5×10^4 low energy electrons (< 20 eV) are produced[3]. These electrons are indeed the most abundant secondary species formed in the interaction of radiation with the biological environment. Subsequent electron capture processes produce considerable damage in isolated nucleobases[4,5,6,7,8], nucleosides[9,10,11] and even DNA adsorbed on surfaces[1,2,12]. The study of the molecular constituents of DNA in the gas-phase, while still a very distant picture from what effectively happens in the physiological environment, can act as a stepping stone towards constructing increasingly encompassing models that are able to explain and predict the real extent of the damage that (non-)ionising radiation imposes upon biological environments. Within this context, the study of methylated variations of thymine and uracil may be perceived as a first step in studying how nucleobase moieties behave when in a molecular DNA framework, rather than in an isolated state. Therefore, the study of these molecules may be considered as one step in expanding the studies from isolated bases to more biologically relevant attuned molecules.

Another major issue regarding the study of the effects of ionising radiation pertains to the more exact nature of the electron capture process, either originating from a free or bound electron, by the (bio) molecular target. Indeed, most of the electron-induced

dissociation studies have been performed by interaction with free electrons. However, while electrons are indeed a major secondary product of ionising radiation, these result from the ionisation of atoms and molecules or are released from their solvated and/or pre-solvated stages within the physiological environment[13,14]. As such, the study of electron transfer processes in atomic collisions with these molecular targets can provide valuable information since the presence of the electron donor can greatly affect the chemical pathways of the reaction.

The present studies focus on the fragmentation channel leading to the loss of a methyl radical triggered by electron transfer in neutral atom-molecule interactions and DEA experiments, briefly represented as:

$$K + MP \rightarrow [K^+(MP^-)]^* \rightarrow K^+ + (MP\text{-}CH_3)^- + CH_3$$

$$e^- + MP \rightarrow (MP^-)^* \rightarrow (MP\text{-}CH_3)^- + CH_3$$

where K stands for a potassium atom and MP a methylated pyrimidine that is either 3-methyluracil (3meU) or 1-methylthymine (1meT). The threshold of anion formation can be obtained from the analysis of mass spectra collected at different collision energies around a particular appearance energy and the possible pathways yielding such fragment negative ion, are proposed by taking advantage of the information provided with the help of the theoretical computations. As far as authors are aware, the mass spectrometric detection of the demethylated anion has never been reported for the presently studied molecules.

Due to the nature of the electron transfer process, and in contrast to free electron attachment studies, the energy of the transferred electron is not precisely fixed and much less known. Generally speaking, the “available” energy for the transferred

electron is dictated by the collision energy in the centre-of-mass frame, meaning that it may be anywhere between ~0 eV and that provided by the collision, as long as that energy matches the energy of a particular unoccupied molecular orbital of the target. As such, any resonance above this value is inaccessible. This may hold at collision energies where only the lowest neutral and ionic states are involved[15], which has been recently reported for selective site- and bond-cleavage in potassium collisions with pyrimidine bases of DNA[16].

2. Experimental

The experimental set-up used in the present studies has already been reported for other pyrimidine related targets[17,18]. Briefly, in the Lisbon laboratory, a hyperthermal neutral potassium beam was formed by accelerating K^+ ions from a source and forcing them to pass through an oven where they resonantly charge exchange with thermal potassium atoms, thereby yielding a neutral hyperthermal potassium beam with an estimated energy resolution of ± 0.5 eV and currents in the order of the pA range for lower energy beams (typically 1pA for 20 eV collision energy). The neutral beam encountered an effusive molecular target in the collision region and upon electron transfer the fragment anions produced were extracted into a Time-of-Flight (TOF) spectrometer and mass analysed. Before reaching the collision area, the neutral potassium beam was monitored by a Langmuir-Taylor ionisation detector, before and after the collection of each spectrum. Mass calibration was carried out on the basis of the well-known anionic species formed after potassium collisions with nitromethane molecule[19]. The extraction region and the TOF system were heated to approximately 393 K throughout measurements in order to prevent any sample condensation and thence charge accumulation on the electrodes. The spectra collected at each collision energy showing the recorded anionic signals, were obtained by subtracting the background signal from the sample signal.

In the Innsbruck experiment, a molecular effusive beam of 1-methylthymine and 3-methyluracil molecules was formed by vaporization of the powder in an electrically heated oven kept in vacuum. The effusive beam of isolated molecules was crossed with an electron beam either in a standard Nier-type ion source[20] or in the collision chamber of an electron monochromator[5]. For the former ion source, the electron current used was about 10 μA with a resolution of about 1 eV (FWHM). Anions formed were accelerated

by 6 kV into the mass spectrometer. After passing a first field-free-region (FF1) anions were analysed by their momentum in a magnetic sector and entered a second field-free-region (FF2). Subsequently anions were analysed by their kinetic energy in an electric sector. The mass and energy analysed anions were detected finally by a channeltron type secondary electron multiplier. In the monochromator setup, the electron current was about 15 nA with a resolution of about 100 meV. Anions formed were extracted by a weak electric field into a quadrupole mass spectrometer and detected by a channeltron type secondary electron multiplier. The temperature used to evaporate the molecules in the oven was about 430 K (sector field mass spectrometer) and 370 K (electron monochromator), respectively.

The 3-methyluracil (3meU) and 1-methylthymine (1meT) solid samples used in the present experiments were purchased from Sigma-Aldrich with a minimum purity of ≥ 99%. They were used as delivered. The samples were heated to 443 K in the Lisbon experiment. In order to test for thermal decomposition products in the target beam, mass spectra were recorded at lower temperatures (from 443 K to 423 K) at the highest collision energy, i.e. 100 eV for 1meT and 50 eV for 3meU, in order to guarantee for a good signal to noise ratio. The ratios between the main fragmentation products appeared unaltered. No other spectra were recorder at higher temperatures.

3. Theoretical methods

The theoretical computations and results presented in this paper are aimed at describing possible pathways that lead to the demethylated negative ion fragments, upon electron attachment to the target molecules, 1-meT and 3-meU. To this purpose, estimates of the relevant temporary anion states need to be considered. As shown in a series of studies by the group of Burrow *et al.*[21], such anion states and the associated vertical attachment energies (VAE) can be predicted in terms of the Koopmans' theorem[22] by calculating the virtual orbital energies (VOE) of the neutral ground state molecule[21,23]. However, VOEs are known to be incorrect in an absolute sense. Hence, empirical scaling functions have been established for certain kind of orbitals (i.e. π^* and σ^* virtual orbitals) to agree with experimental VAE measurements in a group of related compounds, yielding the scaled VOEs (SVOE) for these type of orbitals[24,25].

Thus, following the protocol of Burrow *et al.*[21], 1-meT and 3-meU have been optimized in their neutral electronic and vibrational ground state at the Hartree-Fock level of theory using the double zeta basis set 6-31G(d). The structure and virtual orbitals that are of interest during the demethylation process in 3-meU and 1-meT, respectively, are depicted in Fig. 1 and their SVOEs are listed in Table 1. In Figs. 2 and 3, the potential energy curves (PECs) of these same orbitals are plotted along the N-CH_3 stretching coordinate. The SVOE for the π^*_1-π^*_3 orbitals are then calculated in electron volts (eV) according to $SVOE_{\pi^*} = 0.753\ VOE - 1.968$[26], whereas the scaled $\sigma^*_{N\text{-}CH3}$ orbital energy has been obtained as $SVOE_{\sigma^*} = 0.9\ VOE - 2.55$[27].

In order to estimate possible pathways during the demethylation of both 1-meT and 3-meU, the SVOEs for the π^* and σ^* orbitals have been computed along the demethylation coordinate, that is the 1N-CH_3 distance and the 3N-CH_3 bond distance for 3-meU and 1-meT, respectively (see Figs. 2 and 3), relative to the neutral ground

state energy. For both molecules, a one-dimensional grid of 11 points using different N-C distances between 1.058 Å and 3.058 Å for 1-meT (1.063 Å and 3.063 Å for 3-meU) with a step size of 0.2 Å have been calculated at the HF/6-31G(d) level of theory. The rest of the molecule's framework has been kept frozen at the optimized geometry. For each point on the resulting unrelaxed grid, the relevant wave function characters for the π^*_1-π^*_3 and $\sigma^*_{N\text{-}CH3}$ orbitals have been followed, and SVOEs have been obtained according to the estimation procedure described above. The calculated values, relative to the ground state energy, have been connected using a cubic spline to give a final grid of 1024 points along the dissociation coordinate. Hence, within the Koopmans' theorem, the resulting curves can be considered as an estimation for the diabatic π^* and σ^* anion states for the target molecules.

However, it has to be noted that the used scaling functions have been established to agree with experimental VAEs, which are a measure of the electron attachment energy into a virtual orbital around the ground state minimum geometry. Here, we are considering a significant distortion from that minimum, and hence we cannot be sure if the scaling function is still correct for long N-C distances as it is well known that the computational error of the Hartree-Fock method increases during the description of dissociation processes. Nevertheless, we believe that the obtained curves serve well for a quantitative interpretation of the initial electron attachment (around the ground state minimum) and a qualitative good estimation for the dissociation pathways.

All calculations on 1-meT and 3-meU have been carried out using the GAUSSIAN09 program package[28].

4. Results and discussion

4.1 Electron transfer in potassium-molecule collisions

De-methylated 3-methyluracil $(3meU\text{-}CH_3)^-$

Fig. 4 shows the section ranging from m/z 100 to 130 of a complete TOF mass spectra (not shown here) of the negative ions formed in the collision of potassium atoms with 3-meU. In order to infer on the role of the resonances and the collision dynamics, a set of measurements solely dedicated to studying the $(3meU\text{-}CH_3)^-$ formation were performed, varying the collision energy from 14 eV (5.2 eV available energy) up to 50 eV, vastly above the threshold yielding this anion (see Table 2 for the list of available energies for the different K + MP systems). The dominant fragment anions are the dehydrogenated parent anion (m/z 125), the de-methylated parent anion (m/z 111) and CNO^- (m/z 42). However, of these three fragments, only the dehydrogenated parent anion is present for all collision energies. This is not surprising, given that the formation of this fragment has been assigned to initial access to a π^* state at ~1.8 eV[21], which is lower than 5.2 eV, corresponding to the available energy for K+3meU system at 14 eV collision energy. In contrast, since the presence of CNO^- and $(3meU\text{-}CH_3)^-$ is significantly smaller for 14 eV, it stands to reason that the threshold for the formation of both these channels lies above the corresponding available energy (i.e. 5.2 eV). Indeed, the 14 eV mass spectra in Fig. 4 shows the presence of $(3meU\text{-}H)^-$ but no traces of $(3meU\text{-}CH_3)^-$ which is not discernible from the background baseline. However, for 14.5 eV collision energy (~5.5 eV available energy), formation of $(3meU\text{-}CH_3)^-$ is accessible. This means that $(3meU\text{-}CH_3)^-$ threshold lies between 5.2 and 5.5 eV. Furthermore, it is interesting to note that, for increasing energies, $(3meU\text{-}CH_3)^-$ formation increases, which is rationalized in terms of available energy enabling an increase access to the full width of the resonance profile. In other words, for an

available energy of 9 eV, all of the resonance width may become accessible, whereas for 6 eV only a fraction of the resonance is attainable. Deriving the threshold from the branching ratios turns out to be not possible since, much like $(3meU\text{-}CH_3)^-$ and CNO^- formation are both open at similar thresholds. As such, the branching ratios will not provide the correct information.

A sole study of the experimental data presented herein is, by itself, not able to provide any insight to which mechanism(s) is (are) responsible in the formation of this fragment anion. Theoretical computations of the LUMOs in the ground state were performed in order to help finding the electron densities that ultimately lead to bond breaking upon electron capture. In particular, some of the computed LUMOs were also plotted along the $3N\text{-}CH_3$ coordinate, as presented in Fig. 2. At this point, it is worth stressing that these LUMOs were calculated taking into account solely the neutral ground state of the molecule, i.e. no electronic excited or anion states were considered. As such, no information regarding core-excited resonances can be obtained through the present computations.

From Fig. 2, a vertical transition to the third π* state leads to a transition from the neutral ground state of roughly the same energy as the one obtained in ion-pair formation measurements, which supports accessing a shape resonance. Furthermore, resorting to Fig. 2, a highly antibonding σ* state may be achieved at an energy of ~5.8 eV, which crosses with the aforementioned π* state. This crossing lends support to the proposed pathway of an initial capture to the π* state and subsequent intramolecular electron transfer to the σ* state, leading most likely to dissociation along the $N_3\text{-}CH_3$ bond, yielding the demethylated anion $(3meU\text{-}CH_3)^-$ and a neutral methyl group. This assumption holds as long as the nuclear wavepacket (on the π* configuration) survives long enough to diabatically couple with the repulsive σ* state. Another mechanism is

the direct access to this σ* state. This alternative implies a slightly higher value in vertical electron affinity than the previous pathway and owing to technical reasons, the beam resolution is not enough to unambiguously state which of these pathways is actually accessed.

De-methylated 1-methylthymine (1meT-CH_3)$^-$

Fig. 5 shows the negative ion formation ranging from m/z 105 to 150 from a TOF mass spectrum (not shown here) recorded for 14, 19 and 100 eV potassium collision energies with 1-methylthymine (1-meT) in the lab frame. In Table 2 a list of the corresponding available energies is presented. In contrast to 3-methyluracil, the demethylated fragment can result from abstraction of the methyl group either from the 1N or the 5C positions. In a recent work on potassium-thymine collisions[17], we observed the demethylated parent anion, albeit with a much lower intensity in comparison with the dehydrogenated parent anion. In 1-meT, this fragment is greatly enhanced when compared with the dehydrogenated parent anion, therefore indicating that the majority of the yield stems from CH_3 abstraction from the 1N position. A close inspection of Fig. 5 shows that while at 14 eV there is only a weak evidence of the demethylated parent anion, as the energy is increased its relative yield becomes higher. This indicates that the threshold for formation of this fragment lies very close to 14 eV, which corresponds to ~5.5 eV available energy in the centre-of-mass of the 1meT + K system. From a different point of view, the mechanism yielding such anion formation can be rationalised in terms of the accessible LUMOs (Fig. 1). As such, and following the same procedure as for 3-meU, plotted in Fig. 3 are the accessible π* and σ* states, the latter being dissociative along the 1N-CH_3 bond. A close observation of this figure, and taking into account the fragmentation yields in Fig. 5, leads to two possible mechanisms regarding (1meT-

$CH_3)^-$ formation: a) the electron is initially transferred to the π_3* state and subsequently to the σ* state, which then results in dissociation; or b) direct initial transfer to the σ* state and subsequent dissociation. As in the case of 3meU, the closeness of the vertical transition energies for both states does not allow us to precise which pathway is actually followed, although it is very likely that both should end up in a dissociation through the σ* state.

Finally, formation of the demethylated parent anion in 1-meT could initially be considered to progress along the same pathway as H abstraction from the 1N site in thymine. As has already been shown in free electron attachment studies, H abstraction from the 1N position in thymine (and uracil) proceeds through a Vibrational Feshbach Resonance (VFR) of the dipole-bound anion state, followed by a tunnelling through the potential barrier formed by an avoided crossing between the dipole-bound anion and the lowest dissociative σ* valence state[23,21]. However, methyl abstraction from 1-meT through this mechanism is most likely not possible to happen. Due to the presence of the methyl group, the aforementioned σ* is greatly suppressed along the 1N-CH_3 coordinate thereby inhibiting this fragmentation pathway. In addition, the higher mass of the methyl group, in comparison to the hydrogen atom, will lead to much less efficient tunnelling, as was shown recently in the case of deuteration[29]. Regardless, this is in agreement with the relative quite small yield of the demethylated parent anion appearing below 14 eV collision energy (~5.5 eV available energy). Worth mentioning that such assignment may also accommodate the loss of CH4. However, the calibrations performed for the mass assignments point out systematically to the loss of a CH3. This would benefit in the future from isotopic labelling. One final issue regarding Fig. 5 pertains to the presence of a mass peak assigned to m/z 110 which, due to its broadness and the modest resolution of the TOF mass spectrometer, could also be attributed to m/z

111. Notwithstanding, we do not discard the possibility that this peak may accommodate both anions. Assignment of m/z 111 will most likely consist in the abstraction of C_2H_5, whereas for m/z 110 to C_2H_6 loss. Assuming that these neutral hydrocarbon species are formed from the loss of both methyl groups, m/z 110 would therefore correspond to the abstraction of these two groups, whilst m/z 111 would require a considerable internal rearrangement in the precursor TNI. A more thorough set of calibrations were performed, which tended to point out to the abstraction of C_2H_6.

Another alternative assignment would lead m/z 110 and m/z 111 to COH_2 and COH abstraction, respectively. However, in a previous potassium electron transfer study to thymine[17], we notice a small contribution that corresponds to abstraction of the methyl group from the C5 position (m/z 111), which in the present experiment is an indicative that the feature at m/z 110/111 is due to the loss of two methyl groups.

Regardless, since the present calculations are far beyond the scope of this contribution, this assignment would benefit from further investigation. Regarding the neutral species, we have no information on their molecular structure.

4.2 Dissociative Electron Attachment (DEA) measurements

In addition to the potassium-molecule collisions experiments performed in the Lisbon laboratory, dissociative electron attachment (DEA) experiments with 1-meT and 3-meU were performed in the Innsbruck laboratory regarding the loss of a CH_3 group. Remarkably, also one mass below $(MP\text{-}CH_3)^-$ abundant ion signal is observed, i.e. CH_4 abstraction from both 1meT and 3meU occurs upon free electron capture. In previous DEA experiments with thymine the loss of CH_3 and CH_4 was not observed within the detection limit of the setups used[30] and for 1-meT and 3-meU this reaction channel was not reported yet. The corresponding anion yields as a function of the incident electron energy investigated here for 1-meT and 3-meU are presented in Fig. 6.

Anion formation $(3meU\text{-}CH_3)^-$ & $(3meU\text{-}CH_4)^-$

The anion efficiency curve of $(3meU\text{-}CH_3)^-$ (m/z 111) is shown in Figure 6a measured with the Nier type ion source (energy resolution ~1 eV). Three resonances are observed; the first and most abundant one at ~1.8 eV and two more at ~4 eV and 10.5 eV. The first resonance at 1.8 eV we ascribe to an impurity of the 3meU sample by uracil. DEA studies for uracil have shown that H abstraction from the N_3 site involves a shape resonance at 1.8 eV[31], consisting of an initial occupation of the second π* orbital, followed by an intramolecular electron transfer to the second σ* orbital, which is known to be highly dissociative along the 3N-H stretching coordinate[21,23,31]. We have measured the ion yield shown in Figure 6a also with an energy resolution of about 100 meV utilizing the electron monochromator which allows resolving a sharp vibrational Feshbach resonance observed at 1 eV for uracil and the intensity of the 1.8 eV resonance matches perfectly with that of uracil (U) (not shown). Based on the assumption of the same DEA cross sections for $(U\text{-}H)^-$ and $(3meU\text{-}H)^-$ [31] at 1.8 eV, we

obtain a sample contamination of about 0.7% with uracil. The assignment of the 1.8 eV resonance to an impurity is further supported by the PEC's for 3meU shown in Figure 2. The thermodynamic threshold for formation of $(3meU\text{-}H)^-$ (corresponding to the energy difference between the minimum of the potential energy curve for the neutral ground and the asymptote of the anionic $\sigma^*_{N\text{-}CH3}$ potential energy curve) is about 2.1 eV and hence considerably above the experimental resonance position. Therefore, only the two resonances at higher energies (~4 eV and 10.5 eV) can be ascribed to form upon electron attachment to 3meU. The 4eV resonance can be identified by means of the present SVOE calculations: since population of the third π^* orbital requires electrons with a kinetic energy of more than ~5.3 eV (i.e., 1.3 eV above the DEA resonance maximum), we rather ascribe the dissociation to a direct decomposition process via the purely repulsive second σ^* orbital. It should be noted that the corresponding SVOE at equilibrium distance is about 6 eV. However, this value would correspond to a DEA peak position with neglecting of any autodetachment from the temporary negative ion during dissociation. When including autodetachment the DEA resonance will considerably shift to lower energies[32]. At this point it is critical to note that the accuracy of the calculation of the SVOEs have not been tested thoroughly from an experimental point of view, and as such, these calculations are used in order to provide a tentative assignment between the resonances and the occupied states. The second resonance likely involves a core excited resonance or Rydberg excitation. The lowest electronically excited state of neutral thymine in the gas phase was found at about 3.60 eV and was ascribed to a $\pi \rightarrow \pi^*$ transition[33]. As mentioned above, core excited resonance are not included by the present calculations.

Regarding loss of CH_4, a broad asymmetric resonance is observed, with a threshold at about 4.0 eV, centred at ~7.0 eV and with a yield almost one order of magnitude lower

than the CH_3 abstraction (see Figure 6b). The formation of $(3meU\text{-}CH_4)^-$ requires breaking the N–CH_3 bond and a loss of a hydrogen atom. The resonance maximum is 3 eV lower than the high-energy resonance for CH_3 loss, i.e. a different electronic state of the temporary anion is likely involved. We note that the resonance position is very close to the most abundant peak in the anion yield of CNO^- formed upon DEA to thymine[30]. In the case of electron capture by a pyrimidine base, CNO^- is formed in a two-fold cleavage of the ring and a loss of at least one hydrogen atom from the nitrogen sites. Upon methylation of the N3 position, CNO^- becomes considerable quenched relative to single hydrogen loss: the ratio $(M\text{-}H)^-/CNO^-$ changes to about 12:1 compared to 5:1 for standard thymine[4]. Moreover, the resonance at about 6.8 eV is completely quenched for 3-meT[34]. It is likely that both anions, $(M\text{-}CH_4)^-$ and CNO^- are formed through the same electronic state of the temporary negative ion (TNI) state which is at this electron energy likely a core excited state of the TNI initiating a complex decomposition process including possible molecular rearrangement of the precursor ion.

Concerning the dissociation dynamics we point out that the H abstraction is about a factor of 4 faster than CH_3, i.e. the formation of $(3meU\text{-}CH_4)^-$ can be viewed as a sequential dissociation process, where initially an H is abstracted, followed by the methyl group. Indeed, this fact is supported by a previous study of DEA to thymine embedded in helium droplets, performed in the Innsbruck laboratory, showing that H abstraction is a dissociation intermediate of all other fragments[35]. Fast evaporative cooling in the helium droplet thereby allowed freezing of slow decomposition reactions while $(M\text{-}H)^-$ is formed exclusively due to a fast decomposition along a purely repulsive state of the TNI.

$(1meT\text{-}CH_3)^-$ & $(1meT\text{-}CH_4)^-$

The anion efficiency curves for $(1meT\text{-}CH_3)^-$, m/z 125, & $(1meT\text{-}CH_4)^-$, m/z 124, dissociation channels are shown in Fig. 6c and 6d. The anion efficiency curve for loss of CH_4 consists only of a single resonance centred at ~8.2 eV. We refer again to the ion yield of CNO^- for thymine which shows a resonance at the same energy[30]. The resonance at ~8.2 eV becomes completely suppressed in the ion yield of CNO^- when thymine is methylated at 1N position[34]. Instead $(1meT\text{-}CH_4)^-$ is particularly intense at this resonance energy which follows that after initial H-loss further ligand loss is favoured against ring cleavage. Remarkably the loss of H + CH_3 in the 1-meT anion is more intense than H + H loss in the thymine anion (the difference is a factor of ~16 relative to the corresponding dehydrogenated anion). In the case of twofold hydrogen loss from thymine, the main resonance at high electron energies was found to be at ~7.3 eV. Measurements with partially deuterated thymine showed that this resonance is formed by hydrogen loss from N_1 and N_3[36]. In case of simple (isolated) bond cleavage reactions one would expect a red-shift of the peak position as well as a lower DEA cross section due to increased autodetachment for the loss of H + CH_3. Since both are not observed, we ascribe $(1meT\text{-}CH_4)^-$ to be formed in a complex decomposition process including electronically excited states which are likely to be involved. Methylation alters strongly the relative abundance of the decomposition products formed by this resonant state of the precursor anion.

In contrast to $(1meT\text{-}CH_4)^-$ and the 3-meU molecule, $(1meT\text{-}CH_3)^-$ is not formed in a resonance at higher electron energies; and the ion yield relative to $(1meT\text{-}CH_4)^-$ is much weaker than in the case of 3-meU. The apparent resonance at ~8.2 eV (see Fig. 6c) can be ascribed the ^{13}C isotope contribution of $(1meT\text{-}CH_4)^-$ since the abundance is in perfect agreement with calculated one. Further, $(1meT\text{-}CH_3)^-$ shows low energy

resonances at about 1, 2.1 and 3.7 eV. Based on the calculations of the potential energy diagram for the N-CH_3 reaction coordinate shown in Fig. 3, we may assign the resonances in the following way. The first resonance at about 1 eV arises likely from an impurity since the thermodynamic threshold for production of $(1meT\text{-}CH_3)^-$ is ~1.7 eV (see Fig. 5) and thus above this resonance. The narrow resonance may indicate spurious contamination of the sample with standard thymine (T), since $(T\text{-}H)^-$ with the same nominal mass like $(1meT\text{-}CH_3)^-$ is formed (like uracil) in an intense VFR at 1eV[21]. In DEA to thymine $(T\text{-}H)^-$ has also a resonance at ~ 1.8 eV with about half of intensity of the 1 eV peak. Therefore and in contrast to 3meU, about 70% of the ion yield at the resonance close to 2 eV can be ascribed to result from demethylation of 1meT. The SVOE of the π_2^* orbital is at 1.92 eV, i.e. within the accuracy of experiment and calculations we assign the dissociation process to initial occupation of the π_2^* orbital (see Fig. 3) which couples with the repulsive $\sigma^*_{N\text{-}CH3}$ orbital. The initial occupation of this orbital can be assumed to have a significant overlap with the $\sigma^*_{N\text{-}CH3}$ orbital responsible for the bond break. We note that the thermodynamic threshold for dissociation via $\sigma^*_{N\text{-}CH3}$ orbital is 1.7 eV which allows appearance of this resonance, which is likely not the case for 3meU with a threshold of 2.1 eV. The slightly less abundant peak at 3.9 eV may be explained analogously to the 3meU case, i.e., direct dissociative electron capture into the $\sigma^*_{N\text{-}CH3}$ orbital since the π_3^* orbital is only accessible above 5.6 eV.

4.3 Dissociative Electron attachment vs Ion-pair formation

An issue that is interesting to discuss pertains to the difference between the fragmentation obtained through ion-pair formation and DEA experiments. It is therefore important to highlight a major difference between both set of experiments. This

difference revolves around the intrinsic property of the potassium cation post-collision to suppress electron ejection from the temporary negative ion[17]. Indeed, this auto-detachment suppression mechanism not available in DEA has been shown to exist in electron transfer experiments with nitromethane, as well as in thymine and uracil. In the case of nitromethane, the formation of the parent anion was observed upon electron transfer which is only possible by a suppression of the rejection of the extra electron for long enough time to allow the reaction channel beyond a point where a transition back to the neutral ground state is no longer possible. In contrast, not parent anion was detectable in free electron capture by nitromethane. In thymine and uracil, CNO^- formation in potassium collisions is the dominant channel[17], in contrast to DEA studies where CNO^- only makes up approximately 25% of the total anion yield[4,8]. It was recently proposed that, since the lifetimes of the resonances responsible for this channel are significantly finite, a successful competition with auto-detachment is required. This is accomplished by the presence of the potassium cation[17]. For the case of a metastable transient negative ion, there must be enough time for intramolecular energy distribution through the different available degrees of freedom, yielding a different fragmentation pattern.

For the presently studied methylated compounds we derive that in electron transfer reactions: i) no CH_4 abstraction fragment is obtained; ii) the demethylated parent anion is obtained and, given that the energy threshold for the CH_3 abstraction channel lies at ~5.2 eV, it is very possible that this dissociation pathway consists of an initial electron transfer to one of the σ* or π* orbitals presented in Fig. 1. On the other hand, in DEA no resonance with a threshold at 5 eV is observed while CH_3 abstraction is obtained in a resonance close to 4 eV. The latter energetic difference in the ion yields of DEA and electron transfer is a direct consequence of the substantially lower autodetachment rate

due to the presence of the potassium cation in the collision complex. For example, the ratio of demethylated/dehydrogenated parent anion (the latter being less affected by autodetachment) amounts in DEA to about 0.6 % for 1meT and about 0.1 % for 3meU while in electron transfer these ratios do not hold. Thus the present results show a remarkable modification on the dissociation process due to potassium acting as a stabilizing agent. Compared to an isolated temporary negative ion formed by free electron capture, the anion in the vicinity of a potassium ion favours dissociation rather than autodetachment. We also note that the above mentioned nitromethane case is related to a (metastable) state of the parent anion and CNO^- formation in thymine and uracil represents a rather slow complex dissociation process including rearrangement. In contrast, the demethylation channel studied here is a simple bond cleavage reaction occurring on (much) faster timescales than rearrangement reactions or stabilization of parent anion. One may expect *a priori* for simple bond cleavage reactions that autodetachment to play a less important role than in the case of time consuming reactions which is however not necessarily the case as shown here.

In addition the presence of the potassium cation post-collision changes the structure of the molecular anion which may also lead to the difference in the formation of $(MP-CH_4)^-$ completely absent as product from electron transfer collisions. As mentioned above this anion is formed at the same resonance energy as CNO^- which remains an abundant product in electron transfer collisions while in DEA the channel is quenched.

4. Conclusions

In the work presented here we have investigated negative ion formation in N-site methylated pyrimidine derivatives (3-meU and 1-meT) through atom-molecule collisions, in particular the anionic fragment that results from abstraction of a methyl group from 3meU and 1meT. Additionally, DEA experiments were also performed, with an emphasis on obtaining the ion yields resulting from the CH_3 and CH_4 abstraction in both 3meU and 1meT. The interpretation of the experimental data $(MP\text{-}CH_3)^-$ was complemented with quantum chemical calculations that allowed for the assignment of some of the obtained resonances to the possible initial occupation of σ* and π* orbitals under the assumption that no electronic excitation occurs. This objective was only partially achieved due to the small energy differences of these orbitals inside the Frank-Condon region and the limited energy resolution of the neutral potassium beam. However, generally speaking, the proposed pathways seem to be reasonable to explain the observed fragmentation.

We may also compare the present results for 1meT with the nucleoside thymidine where the nucleobase and sugar moiety are linked at the 1N site by the glycosidic bond. A previous DEA study with thymidine indeed reported the glycosidic bond cleavage[9]. The resulting ion yield of the negatively charged thymine moiety showed lower-energy resonances below 3 eV as well as two resonances at 6.6 eV and 7.8 eV. While the lower-energy resonances (< 3 eV) were mostly shown to result from DEA to the thermal decomposed products (with the exception of a small contribution at virtually no energy which was ascribed to an impurity[9]), the higher energy features are indeed due to DEA to the pristine molecule[9]. Since here we observe for $(1meT\text{-}CH_3)^-$ only low energy resonances and no high energy resonance, the DEA channel leading to the 1N-C bond cleavage becomes substantially modified when going to the methylated nucleobase to

thymidine. This indicates the limitation of the present molecules as model compounds for nucleosides at least for DEA. In contrast, a recent study on esterification of amino-acids has shown that methylation in the carboxyl group of amino-acids, in comparison to esterification with larger alkyl groups, does not seem to greatly change the negative fragment ion formation[37].

Finally, one can argue that, given the ability of electron transfer processes to strongly lower autodetachment rates and therefore enhance fragmentation channels, these processes may have a more damaging effect on biological molecules than DEA. In the latter case auto-detached electrons will, at most, leave the molecule in a non-dissociative vibrationally excited state.

Acknowledgments

DA and FFS acknowledge the Portuguese Foundation for Science and Technology (FCT-MEC) for post-graduate and post-doctoral scholarships SFRH/BD/61645/2009 and SFRH/BPD/68979/2010, respectively. DA acknowledges the valuable discussions with Dr. Rodrigo Antunes and Eng. Gonçalo Martins. PL-V, FFS and DA acknowledge the strategic grant PEst-OE/FIS/UI0068/2011. PL-V and GG acknowledge the support from the Portuguese-Spanish joint collaboration through the bilateral Project HP 2006-0042. This work also forms part of EU/ESF COST Actions The Chemical Cosmos CM0805 and Nanoscale Insights into Ion Beam Cancer Therapy (Nano-IBCT) MP1002. This work was partially supported by the Fonds zur Förderung der wissenschaftlichen Forschung (FWF, P22665), Wien.

References

1. B. Boudaïffa, P. Cloutier, D. Hunting, M. A. Huels, and L. Sanche, Science, 2000, 287, 1999–2001.

2. F. Martin, P. Burrow, Z. Cai, P. Cloutier, D. Hunting, and L. Sanche, Phys. Rev. Lett., 2004, 93, 6–9.

3. V. Cobut, Y. Frongillo, J. P. Patau, and T. Goulet, Radiat. Phys. Chem., 1998, 3, 229–243.

4. S. Denifl, S. Ptasinska, M. Cingel, S. Matejcik, P. Scheier, and T. D. Märk, J. Chem. Phys., 2003, 377, 74–80.

5. S. Denifl, P. Sulzer, D. Huber, F. Zappa, M. Probst, T. D. Märk, P. Scheier, N. Injan, J. Limtrakul, R. Abouaf, and H. Dunet, Angew. Chem., Int. Ed. Engl., 2007, 46, 5238–41.

6. I. Baccarelli, I. Bald, F. a. Gianturco, E. Illenberger, and J. Kopyra, Phys. Rep., 2011, 508, 1–44.

7. E. Alizadeh and L. Sanche, Chem. Rev., 2012, 112, 5578-5602.

8. S. Denifl, S. Ptasińska, G. Hanel, B. Gstir, M. Probst, P. Scheier, and T. D. Märk, J. Chem. Phys., 2004, 120, 6557–65.

9. S. Ptasińska, S. Denifl, S. Gohlke, P. Scheier, E. Illenberger, and T. D. Märk, Angew. Chem., Int. Ed. Engl., 2006, 45, 1893–6.

10. H. Abdoul-Carime, S. Gohlke, E. Fischbach, J. Scheike, and E. Illenberger, Chem. Phys. Lett., 2004, 387, 267–270.

11. S. Denifl, P. Candori, S. Ptasińska, P. Limão-Vieira, V. Grill, T. D. Märk, and P. Scheier, Eur. Phys. J. D, 2005, 35, 391–398.

12. S. V. K. Kumar, T. Pota, D. Peri, A. D. Dongre, and B. J. Rao, J. Chem. Phys., 2012, 137, 045101.

13. L. Sanche, Nature, 2009, 461, 358.

14. C. Wang, J. Nguyen, and Q. Lu, J. Am. Chem. Soc., 2009, 131, 11320–2.

15. A. W. Kleyn and A. M. C. Moutinho, J. Phys. B: At. Mol. Opt. Phys., 2001, 4075, R1-R44.

16. D. Almeida, F. Ferreira da Silva, G. Garcia, and P. Limão-Vieira, Phys. Rev. Lett, 2013, 110, 023201.

17. D. Almeida, R. Antunes, G. Martins, S. Eden, F. Ferreira da Silva, Y. Nunes, G. Garcia, and P. Limão-Vieira, Phys. Chem. Chem. Phys., 2011, 13, 15657–65.

18. F. Ferreira da Silva, D. Almeida, R. Antunes, G. Martins, Y. Nunes, S. Eden, G. Garcia, and P. Limão-Vieira, Phys. Chem. Chem. Phys., 2011, 13, 21621–9.

19. R. Antunes, D. Almeida, G. Martins, N. J. Mason, G. Garcia, M. J. P. Maneira, Y. Nunes, and P. Limão-Vieira, Phys. Chem. Chem. Phys., 2010, 12, 12513–9.

20. D. Huber, M. Beikircher, S. Denifl, F. Zappa, S. Matejcik, A. Bacher, V. Grill, T. D. Märk, and P. Scheier, J. Chem. Phys., 2006, 125, 084304.

21. P. D. Burrow, G. A. Gallup, A. M. Scheer, S. Denifl, S. Ptasinska, T. Märk, and P. Scheier, J. Chem. Phys., 2006, 124, 124310.

22. T. Koopmans, Physica, 1934, 1, 104–113.

23. A. M. Scheer, K. Aflatooni, G. Gallup, and P. Burrow, Phys. Rev. Lett., 2004, 92, 3–6.

24. D. Chen and G. A. Gallup, J. Chem. Phys., 1990, 93, 8893.

25. N. Heinrich, W. Koch, and G. Frenking, Chem. Phys. Lett., 1986, 124, 20-25.

26. K. Aflatooni, G. A. Gallup, and P. D. Burrow, J. Chem. Phys., 2010, 132, 094306.

27. K. Aflatooni and P. D. Burrow, J. Chem. Phys., 2000, 113, 1455.

28. M. J. Frisch, G. W. Trucks, H. B. Schlegel, G. E. Scuseria, M. A. Robb, J. R. Cheeseman, G. Scalmani, V. Barone, B. Mennucci, G. A. Petersson, H. Nakatsuji, M. Caricato, X. Li, H. P. Hratchian, A. F. Izmaylov, J. Bloino, G. Zheng, and D. J. Sonnenb, Gaussian 09, Revision A.1, 2009.

29. S. Denifl, P. Sulzer, F. Zappa, S. Moser, B. Kräutler, O. Echt, D. K. Bohme, T. D. Märk, and P. Scheier, Int. J. Mass Spectrom., 2008, 277, 296–299.

30. S. Denifl, S. Ptasińska, M. Probst, and J. Hrus, J. Phys. Chem. A, 2004, 6562–6569.

31. S. Ptasinska, S. Denifl, P. Scheier, E. Illenberger, and T. D. Märk, Angew. Chem., Int. Ed. Engl., 2005, 44, 6941–6943.

32. V. Vizcaino, B. Puschnigg, S. E. Huber, M. Probst, I. I. Fabrikant, G. A. Gallup, E. Illenberger, P. Scheier, and S. Denifl, New J. Phys., 2012, 14, 043017.

33. R. Abouaf, J. Pommier, and H. Dunet, Chem. Phys. Lett., 2003, 381, 486–494.

34. F. Ferreira da Silva, C. Matias, D. Almeida, G. García, O. Ingólfsson, H. D. Flosadottir, S. Ptasińska, B. Puschnigg, P. Scheier, P. Limão-Vieira, and S. Denifl, In preparation, 2012.

35. S. Denifl, F. Zappa, A. Mauracher, F. F. da Silva, A. Bacher, O. Echt, T. D. Märk, D. K. Bohme, and P. Scheier, Chem. Phys. Chem., 2008, 9, 1387–1389.

36. S. Ptasińska, S. Denifl, B. Mróz, M. Probst, V. Grill, E. Illenberger, P. Scheier, and T. D. Märk, J. Chem. Phys., 2005, 123, 124302.

37. Y. V. Vasil'ev, B. J. Figard, D. F. Barofsky, and M. L. Deinzer, Int. J. Mass Spectrom., 2007, 268, 106–121.

Figure captions

Figure 1 – Structure and virtual orbitals of π* character as well as of σ* character along the N-CH_3 coordinate of the neutral 1meT and 3meU molecules obtained at the HF/6-31G* level of theory.

Figure 2 – Plot of the 3meU SVOEs for the second and third π* orbitals (red) as well as of the σ* orbital (blue), presented in Fig. 1, along the N-CH_3 stretching coordinate relative to the neutral ground state energy (black). VOEs and ground state energy have been obtained at the HF/6-31G* level of theory; scaling of VOEs has been done according to description in text.

Figure 3 – Plot of the 1meT SVOEs for the second and third π* orbitals (red) as well as of the σ* orbital (blue), presented in Fig. 1, along the N-CH_3 stretching coordinate relative to the neutral ground state energy (black). VOEs and ground state energy have been obtained at the HF/6-31G* level of theory; scaling of VOEs has been done according to description in text.

Figure 4 – Negative ion TOF mass spectra for potassium collisions with 3meU at 14, 14.5, 15.5, 30 and 50 eV in the lab frame. Arbitrary units result from the anionic signal divided by the potassium beam current and accumulation time.

Figure 5 – Negative ion TOF mass spectra for potassium collisions with 1meT at 14, 19 and 100 eV in the lab frame. Arbitrary units result from the anionic signal divided by the potassium beam current and accumulation time.

Figure 6 – DEA resonance profiles for formation of a) $(3meU\text{-}CH_3)^-$, b) $(3meU\text{-}CH_4)^-$, c) $(1meT\text{-}CH_3)^-$ and d) $(1meT\text{-}CH_4)^-$. Measurements shown in a), b) and d) were derived utilizing the Nier type ion source (energy resolution ~1 eV) while for c) the electron monochromator was used (resolution ~0.1 eV).

Table captions

Table 1 – Scaled virtual orbital energies (SVOEs) from HF/6-31G* calculations for the optimized neutral equilibrium molecules (see Fig. 1), in eV.

Table 2 – Table of available energies for the different collision energies. The energy resolution of the beam will be, for all collision energies, 0.5 eV.

Figure 1

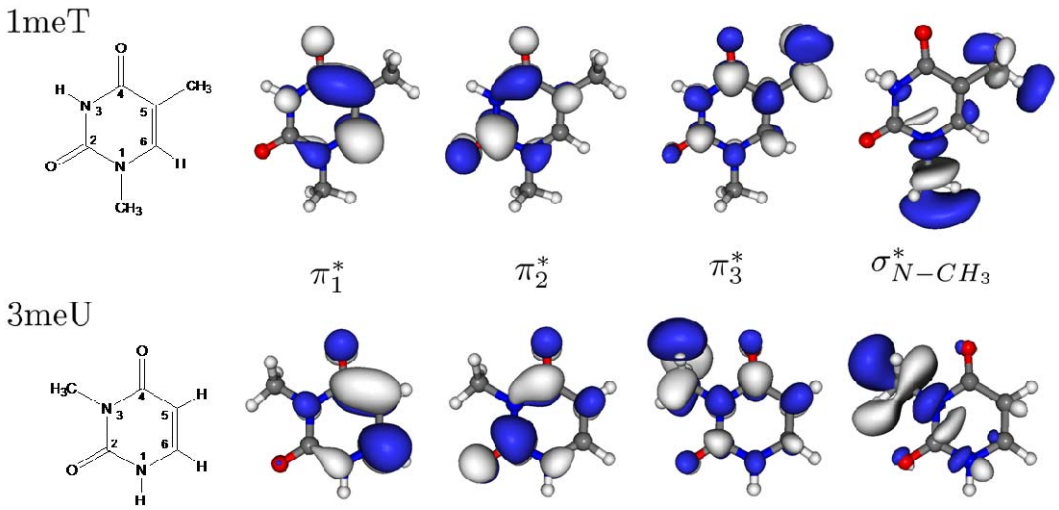

Figure 2

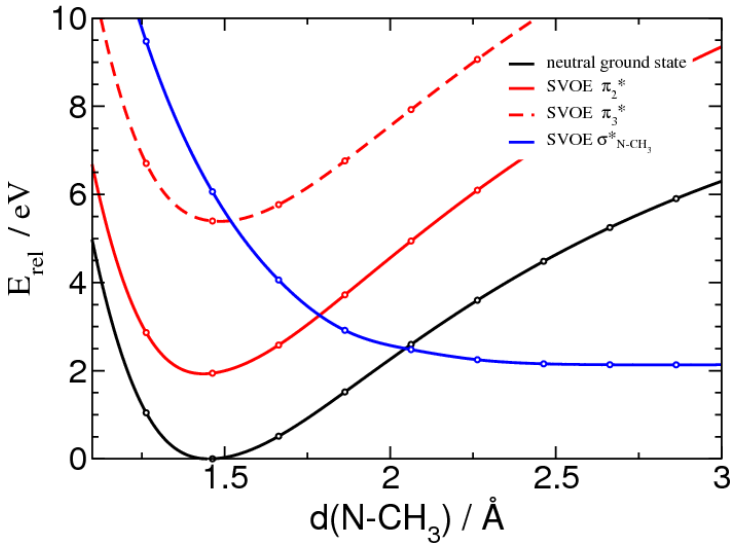
10
8
6
4
2
0
1.5
2
2.5
3
E_rel / eV
d(N-CH3) / Å
neutral ground state
SVOE π2*
SVOE π3*
SVOE σ*N-CH3

Figure 3

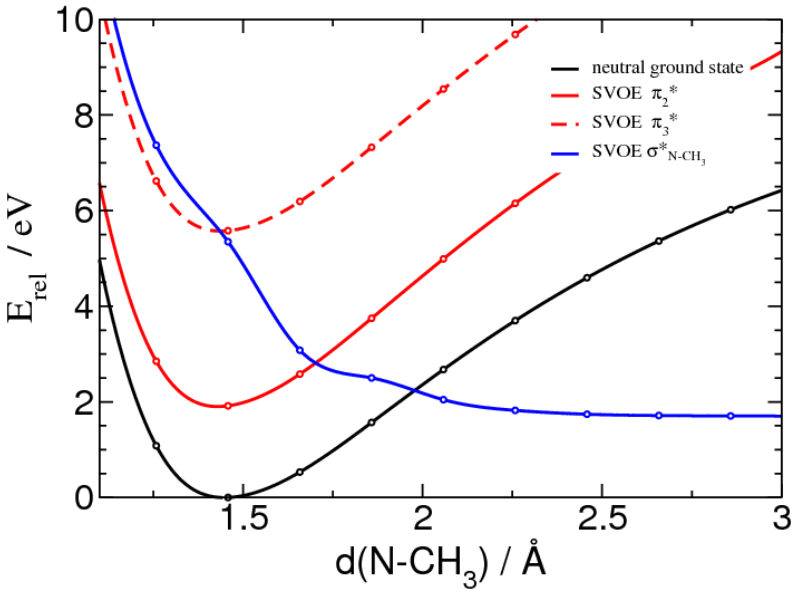
neutral ground state
SVOE π2*
SVOE π3*
SVOE σ*N-CH3
Erel / eV
d(N-CH3) / Å
0
2
4
6
8
10
1.5
2
2.5
3

Figure 4

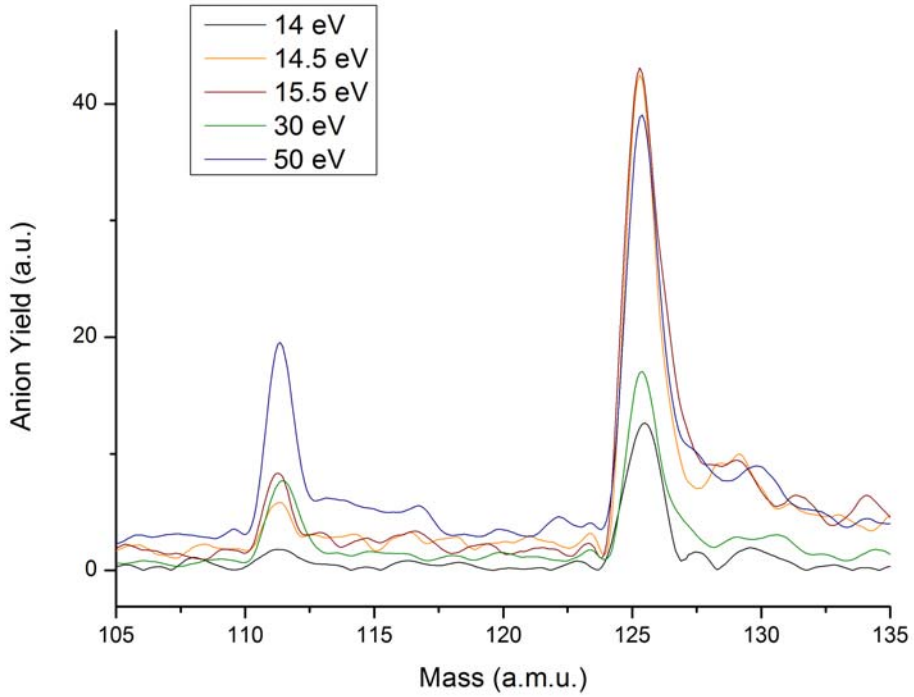
14 eV
14.5 eV
15.5 eV
30 eV
50 eV
Anion Yield (a.u.)
0
20
40
105
110
115
120
125
130
135
Mass (a.m.u.)

Figure 5

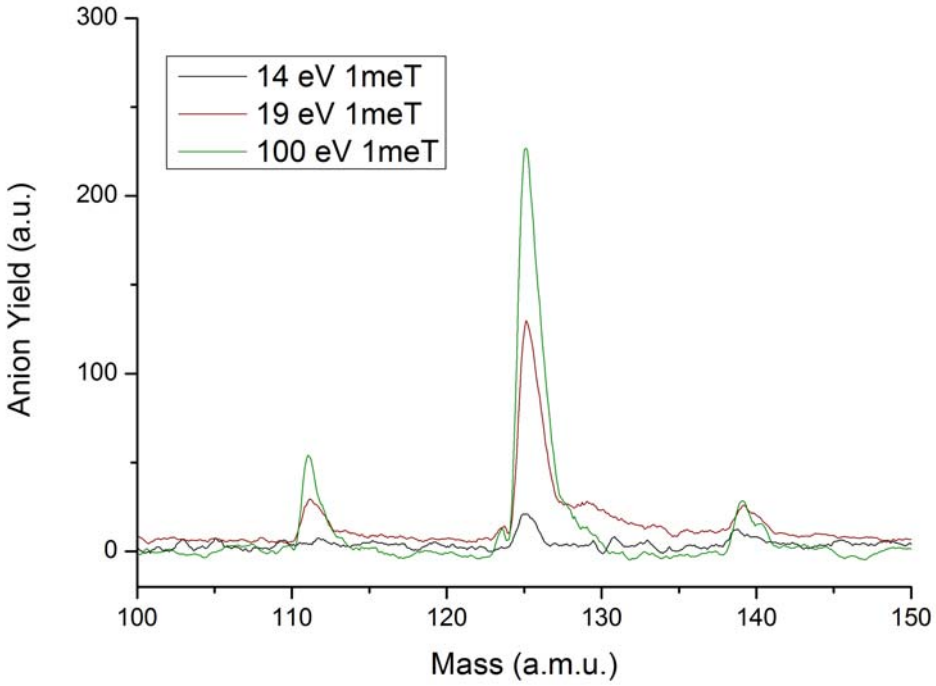
14 eV 1meT
19 eV 1meT
100 eV 1meT
Anion Yield (a.u.)
300
200
100
0
100
110
120
130
140
150
Mass (a.m.u.)

Figure 6

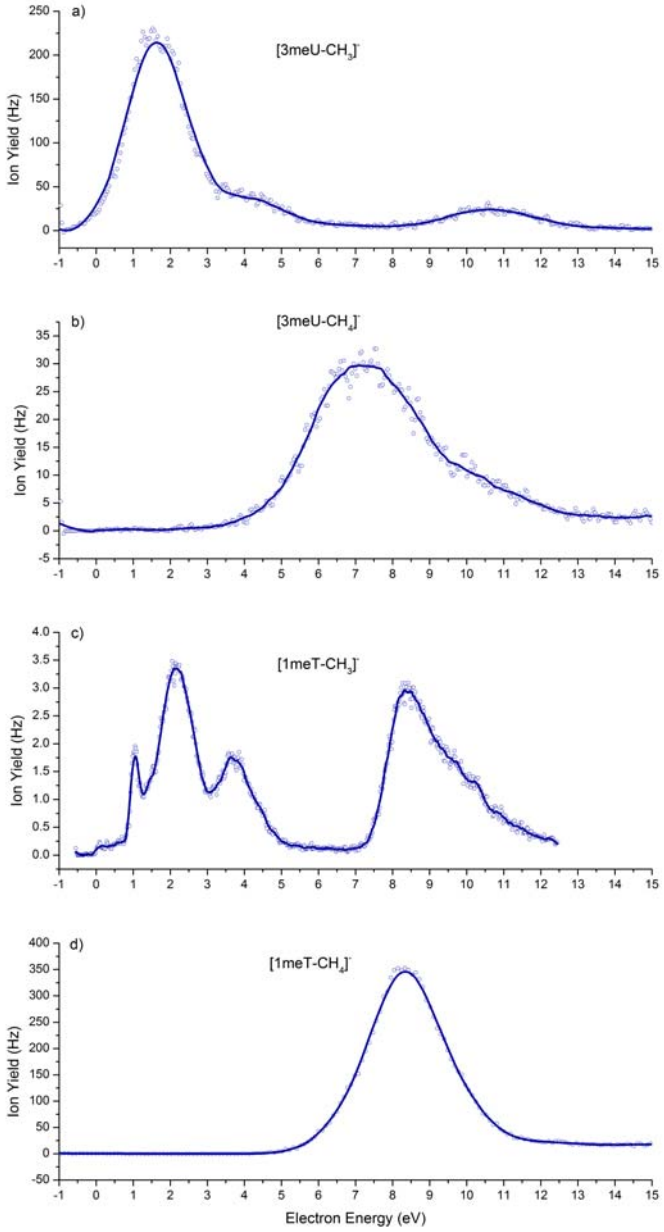
a)
[3meU-CH3]-
b)
[3meU-CH4]-
c)
[1meT-CH3]-
d)
[1meT-CH4]-
Ion Yield (Hz)
Electron Energy (eV)

Table 1

Compound	π_1*	π_2*	π_3*	σ*(N-CH_3)
3meU	0.40	1.94	5.39	6.06
1meT	0.48	1.91	5.58	5.35

Table 2

Collision energy in the lab frame (eV)	Available energy (eV)	
	3meU	1meT
14.0	5.2	5.5
14.5	5.5	-
15.5	6.2	-
19.0	-	9.0
30.0	16.0	-
50.0	29.6	-
100.0	-	66.1